Atmos. Chem. Phys. Discuss., doi:10.5194/acp-2017-74, 2017
Manuscript under review for journal Atmos. Chem. Phys.
Discussion started: 9 March 2017

Atmospheric Chemistry and Physics Discussions
Open Access

Projected global tropospheric ozone impacts on vegetation under different emission and climate scenarios

Sicard Pierre[1], Anav Alessandro[2], De Marco Alessandra[3], Paoletti Elena[2]

[1] ACRI-HE, Sophia Antipolis, France
[2] Institute of Sustainable Plant Protection, National Research Council, Sesto Fiorentino, Italy
[3] Italian National Agency for New Technologies, Energy and the Environment, C.R. Casaccia, Italy

Abstract

The impact of ground-level ozone (O_3) on vegetation is largely under-investigated at global scale despite worldwide large areas are exposed to high surface O_3 levels and concentrations are expected to increase in the next future. To explore future potential impacts of O_3 on vegetation, we compared historical and projected O_3 concentrations simulated by six global atmospheric chemistry transport models on the basis of three representative concentration pathways emission scenarios (i.e. RCP 2.6, 4.5, 8.5). To assess changes in the potential O_3 threat to vegetation, we used the AOT40 metric. Results point out a significant overrun of AOT40 in comparison with the recommendations of UNECE for the protection of vegetation. In fact, many areas of the northern hemisphere show that AOT40-based critical levels will be exceeded by a factor of at least 10 under RCP8.5. Changes in surface O_3 by 2100 range from about + 4-5 ppb worldwide in RCP8.5 scenario to reductions of about 2-10 ppb in the RCP2.6 scenario. The risk of O_3 injury for vegetation decreased by 61% and 47% under RCP2.6 and RCP4.5, respectively and increased by 70% under RCP8.5. Key biodiversity areas in South and North Asia, central Africa and Northern America were identified as being at risk from high O_3 concentrations. To better evaluate the regional exposure of ecosystems to O_3 pollution, we recommend the use of improved chemistry-climate modelling system, fully coupled with dynamic vegetation models.

* Corresponding author: pierre.sicard@acri-he.fr

Keywords: AOT40, Ozone, Representative Concentration Pathways, O_3 injury on vegetation

Introduction

Tropospheric ozone (O_3) is a secondary air pollutant, i.e. it is not emitted as such in the air but it is formed by reactions among precursors (e.g. CH_4, VOCs, NOx). Ozone is an important greenhouse gas resulting in a direct radiative forcing of 0.35-0.37 W m^{-2} on climate (Shindell et al., 2009; Ainsworth et al., 2012). Despite significant control efforts and legislation to reduce O_3 precursor emissions, tropospheric O_3 pollution is still a major air quality issue over large regions of the Globe (Lefohn et al., 2010; Langner et al., 2012; Young et al., 2013; Cooper et al., 2014; EEA, 2015; Sicard et al., 2016a,b). Long-range transport of O_3 and its precursors can elevate the local and regional O_3 background concentrations (Ellingsen et al., 2008; Wilson et al., 2012; Paoletti et al., 2014; Derwent et al., 2015; Xing et al., 2015; Sicard et al., 2016a). Therefore, remote areas such as the Arctic region, can be affected (Langner et al., 2012). The current tropospheric O_3 levels (35-50 ppb in the northern hemisphere, NH) are high enough to damage both forests and crops by reducing growth rates and productivity (Paoletti et al, 2009; Wittig et al., 2009; Anav et al., 2011; Mills et al., 2011; Ashworth et al., 2013; Proietti et al., 2016).

Increasing atmospheric CO_2, nitrogen deposition and temperatures enhance plant growth, and increase primary production and greening of plants (Nemani et al., 2003; Zhu et al., 2016). At the global scale, a widespread increase of greening and net primary production (NPP) is observed over 25-50% of the vegetated area, while a decrease is observed over only 7% of the Globe (Nemani et al., 2003; Zhu et al., 2016). In contrast, a previous modeling study over Europe shows how O_3 reduces the mean annual gross primary production (GPP) by about 22% and the leaf area index by 15-20% (Anav et al., 2011). Similarly, Proietti et al (2016), using different *in-situ* measurements collected over 37 European forest sites, found a GPP decrease of 30% caused by O_3. At global scale, over the time period 1901-2100, GPP is projected to decrease by 14-23% (Sitch et al., 2007). As a consequence of reduced photosynthetic assimilation, the total biomass of trees is estimated to be decreased by 7% under the current O_3 mean concentrations (40 ppb) and by 17% under the O_3 mean concentrations expected in 2100 (97 ppb) compared to preindustrial O_3 levels (about 10 ppb, Wittig et al., 2009). Wittig et al. (2009) also reported that the total tree biomass of angiosperms was reduced by 23% at O_3 mean concentrations of 74 ppb, and by 7% at 92 ppb for gymnosperms. High surface O_3 levels, exceeding 40 ppb, do occur in many regions of the Globe with associated economic costs of several billion dollars per year (Wang and Mauzerall, 2004; Ashmore, 2005). Ashworth et al. (2013) reported an annual loss of 3.5% for wheat (very O_3-sensitive) and 1% for maize (more O_3-tolerant) for Europe in 2010 relative to 2000, while Holland et al. (2006) estimated a €4.5 billion loss in the production of 23 common crop species, due to surface O_3 exposure by 2020 relative to 2000.

The international Tropospheric Ozone Assessment Report (TOAR) establishes a state-of-the-art and an up-to-date scientific assessment of global O_3 metrics for climate change, human health and crop/ecosystem research (Lefohn et al. 2017). To assess the potential O_3 risk and protect vegetation from O_3, different metrics are used: the European and US standard (AOT40 and W126, respectively) are based on exposure-based metrics, while flux-based metrics have been introduced only recently (UNECE, 2010; Klingberg et al., 2014; EEA, 2015). Unlike the exposure-based metrics, which only rely on the surface O_3 concentration, the flux-based metrics were developed to quantify the accumulation of damaging O_3 taken up by vegetation through the stomata over a species-specific phenological time-window. These metrics also provide an information-rich tool in assessing the relative effectiveness of air pollution control strategies in lowering surface O_3 levels worldwide (Monks et al., 2015). By reducing plant photosynthesis and growth, high tropospheric O_3 levels will result in reduction in carbon storage by vegetation and, *in fine* an indirect radiative forcing as a consequence of the CO_2 rising in the atmosphere (Sitch et al., 2007; Ainsworth et al., 2012). This CO_2 rising reduces stomatal conductance which decreases O_3 flux into plants leading to increased O_3 levels in the air of 3-4 ppb during the growing season over the NH by doubling of CO_2 concentration (Fiscus et al., 2005; Sanderson et al., 2007).

Projected changes in tropospheric O_3 vary considerably among models (Stevenson et al., 2006; Wild, 2007) and emission scenarios. In earlier studies, the emissions of O_3 precursors were based on a high population growth, leading to very high projected surface O_3 concentrations by 2100 (Stevenson et al., 2000; Zeng and Pyle, 2003; Shindell et al., 2006). The last emission scenarios, i.e. the Representative Concentration Pathways (RCPs) were developed as part of the Fifth Assessment Report of the Intergovernmental Panel on Climate Change (Meinshausen et al., 2011; van Vuuren et al., 2011; Cubasch et al., 2013; Myhre et al., 2013). These scenarios include e.g. different assumptions on climate, energy access policies, and land cover and land use changes (Arneth et al., 2008; Kawase et al., 2011; Kirtman et al., 2013). Until now, studies on O_3 pollution impacts on terrestrial ecosystems are either limited to a single model or to particular regions (e.g. Clifton et al., 2014; Rieder et al., 2015) and only a few applications of global or regional models under the new RCPs scenarios were carried out (Kelly et al., 2012). In the framework of the Atmospheric Chemistry and Climate Model Intercomparison Project (ACCMIP), different simulations were performed by Lamarque et al. (2013) and Young et al. (2013) from 16 global chemistry models.

A few issues about surface O_3, such as a better understanding of spatial changes and a better assessment of O_3 impacts worldwide, are still challenging. To overcome these issues, the aim of this study is to quantify, for the first time, the spatial and temporal changes in the projected potential O_3 impacts on carbon assimilation of vegetation at global scale, by comparing the O_3 potential injury at present with that expected at the end of the 21st century from different global chemistry models.

Materials and Methods

ACCMIP models and RCP scenarios

The global chemistry models used in this work have been developed under the ACCMIP project. A detailed description of the selected models and of the emission scenarios (i.e. RCPs) is included in Supplementary Information (SI). ACCMIP models have been widely validated and used to evaluate projected changes in atmospheric chemistry and air quality under different emission and climate assumptions (e.g. Lamarque et al., 2010; Fiore et al., 2012; Bowman et al., 2013; Lee et al., 2013; Voulgarakis et al., 2013). Lamarque et al. (2013) and Young et al. (2013) provided the main characteristics of 16 models and details for the ACCMIP simulations. Although within the ACCMIP project 16 models are available, due to the lack of hourly O_3 concentration here we only focus on 6 global chemistry models with different configurations (Table 1).

The length of historical and RCP simulations vary between models, but for all models the historical runs cover a period centered around 2000, while the time-slice of RCPs is centered around 2100 (Table 1). As for each model we compare the mean change between the historical and RCP simulations, a different length in the number of years used in the analysis does not affect the results.

Potential ozone injury on vegetation

The O_3 exposure-based index, i.e. AOT40 (ppb h), is a metric used to assess the potential O_3 risk to vegetation from local to global scales (Emberson et al., 2014). It is computed as sum of the hourly exceedances above 40 ppb, for daylight hours (8am-8pm) over species-specific growing seasons (UNECE, 2010). A recent study over Europe showed how computing AOT40 only over the growing season (i.e. April-September) would lead to an underestimation of AOT40 up to 50% for conifer trees, while in case of deciduous trees the underestimation is much smaller (< 5%, Anav et al., 2016). Besides, it should be noted that in Anav et al. (2016) the AOT40 is computed year-round when the stomatal conductance is greater than 0. Here, because of the lack of hourly meteorological data, we can only compute the AOT40 year-round and during the daylight hours. In case of risk assessment, this approach would lead to a relevant overestimation of AOT40, mainly over polluted area of NH. Nevertheless, since the aim of this study is to compare how O_3 stress to vegetation changes between historical period and future, the overestimation of AOT40 does not affect our results. Therefore, we computed AOT40 as follows:

$$AOT40 = \int_{01jan}^{31dec} \max\left(\left([O_3] - 40\right), 0\right).dt \qquad (1)$$

where $[O_3]$ is hourly O_3 concentration (ppb) simulated by the models at the lower model layer and *dt* is time step (1h). The function "maximum" ensures that only values exceeding 40 ppb are taken into account. The O_3 concentration to be used in AOT40 calculation should be at the top of the canopy; however, most of models used here provide O_3 concentrations at 90-120 m. Nevertheless, even if the O_3 concentration is simulated at different elevations above the sea level, as for each model we compare the variation between present and future, the change is consistent because the elevation is the same. For the protection of forests, a critical level of 5,000 ppb.h (or 5 ppm.h) is recommended by UNECE (2010). Within the 2008/50/CE Directive, the critical level for agricultural crops (3 ppm.h) is adopted as the long-term objective value for the protection of vegetation by 2020.

From the AOT40, a factor of risk for forests and crops can be computed (Anav et al. 2011; Proietti et al. 2016). Thus, the potential O_3 impact on photosynthetic assimilation (IO_3) is expressed as following:

$$IO3 = \alpha \times AOT40 \qquad (2)$$

where α is an empirically derived O_3 response coefficient representing the proportional change in photosynthesis per unit of ozone-uptake (Anav et al., 2011). The coefficient for coniferous trees (0.7×10^{-6} mm^{-1} ppb^{-1}) and crops (3.9×10^{-6} mm^{-1} ppb^{-1}) are based on the regressions of the ozone-uptake response curves (Reich, 1987), while the coefficient for deciduous trees and other vegetation types (2.6×10^{-6} mm^{-1} ppb^{-1}) is based on Ollinger et al. (1997). From changes in the risk factor, we can highlight potential risk areas for vegetation.

Results and Discussion

Although differences in the simulated global O_3 spatial pattern were previously discussed and analyzed (e.g. Lamarque et al., 2013), we show the mean annual O_3 concentration at the lower model layer in Figure 1 because O_3 concentration explains AOT40 patterns. Then, in Figure 2 we show and discuss the AOT40 spatial and temporal distribution from the ACCMIP models for the historical and RCPs simulations, and finally in Figure 3 we show the percentage of variation of IO3, i.e. the change in the potential impact of O_3 on vegetation for the ACCMIP models computed comparing the RCPs simulations with historical runs. A detailed description of each figure, model by model, is included in Supplementary Information (SI).

Spatial pattern of historical ozone concentration and AOT40

The highest surface O_3 concentrations (Fig. 1) and potential O_3 injury (Fig. 2) are found in the NH, highlighting a hemispheric asymmetry. The multi-models O_3 mean concentration, averaged over the land points of the domain, is 37.9 ± 4.3 ppb in NH and 22.9 ± 3.8 ppb in SH (Table 3a). The NH extratropics (i.e. mid-latitudes beyond the tropics) has 65% more O_3 than the SH extratropics (data not shown). The highest AOT40 values are found in the NH, with an averaged AOT40 of 24.8 ± 10.1 ppm.h in NH and 2.5 ± 1.7 ppm.h in SH (Table 3a).

According to previous studies, the annual mean background O_3 concentrations at NH mid-latitudes range between 35 and 50 ppb during the end of the 20th century (e.g. Cooper et al., 2012; IPCC, 2014; Lefohn et al. 2014). Similarly, we found historical surface O_3 mean concentrations ranging between 35 and 50 ppb and 35-50 ppm.h for AOT40 in the NH, with the highest values occurring over Greenland and in the latitude band 15-45°N, particularly around the Mediterranean basin, Near East, Northern America and over the Tibetan plateau (> 50 ppb and 70 ppm.h) while the lowest O_3 burden (15-30 ppb, < 20 ppm.h) was recorded in SH, particularly over Amazon, African and Indonesian rainforests. Tropospheric O_3 has a significant source from stratospheric O_3 (Parrish et al., 2012) and it can be transported by the large-scale Brewer-Dobson overturning circulation, i.e. an upward motion from the tropics and downward at higher latitudes, resulting in higher O_3 concentrations in the extratropics

(Hudson et al., 2006; Seidel et al., 2008; Parrish et al., 2012). The six models are able to reproduce the spatial pattern of O_3 concentration and thus AOT40 worldwide.

The highest historical O_3 mean concentrations are observed in GFDL-AM3 and the lowest are found in MIROC-CHEM. In the early 2000s, the maximum global O_3 mean concentration (39 ppb) in GFDL-AM3 is associated to the lowest annual total NOx emissions (46.2 Tg, Table 2a) and low LNOx (4.4 Tg) while the minimum global O_3 mean concentration (28 ppb) in MIROC-CHEM is related to the highest emissions of total NOx per year (57.3 Tg) and erroneously high LNOx (9.7 Tg per year, Lamarque et al., 2013). MIROC-CHEM simulates 58 gaseous species in the chemical scheme with constant present-day biogenic VOCs emissions while GFDL-AM3 simulates 81 species (Stevenson et al., 2012; Lamarque et al., 2013). In GISS-E2-R, the hemispheric asymmetry in O_3 is more important with e.g. a mean concentration of 22 ppb in SH and 42 ppb in NH. A stronger global AOT40 mean (26 ppm.h) is observed in GISS-E2-R and the lowest (7 ppm.h) in MIROC-CHEM for historical simulations. Model-to-model differences are observed due to different natural emissions of O_3 precursors (e.g. lightning NOx) and the used chemical schemes.

Higher O_3 burdens (mean concentration > 50 ppb, AOT40 >70 ppm.h) are simulated at high-elevation areas, e.g. at Rocky and Appalachian Mountains and over the Tibetan plateau (Fig. 1, Fig. 2).At high-elevation, solar radiation, biogenic VOC emission, exchange between free troposphere and boundary layer, and stratospheric O_3 intrusion within the troposphere are more important that at the surface layer (Steinbacher et al. 2004; Kulkarni et al., 2011; Lefohn et al., 2012). Altitude reduces the O_3 destruction by deposition and NO (Chevalier et al., 2007). In addition, due to the high elevation, ambient air remains colder and dryer in summer, leading to lower summertime O_3 losses from photolysis (Helmig et al., 2007). The high-elevation areas, characterized by higher O_3 burdens, are well simulated in GISS-E2-R and MOCAGE models.

The Tibetan plateau, so-called “ozone valley”, is the highest plateau in the world, with a mean height of 4000 m a.s.l. (Tian et al., 2008) with strong thermal and dynamic influences on regional and global climate (Chen et al. 2011). High surface O_3 mean concentrations (40-60 ppb) were reported in previous studies (e.g. Zhang et al., 2004; Bian et al., 2011; Guo et al., 2015; Wang et al., 2015). Although this region is remote, road traffic, biofuel energy source, coalmines and trash burning are prevalent. These pollution sources contribute to significant

Atmos. Chem. Phys. Discuss., doi:10.5194/acp-2017-74, 2017
Manuscript under review for journal Atmos. Chem. Phys.
Discussion started: 9 March 2017

amount of NOx, CO and VOCs (Wang et al., 2015). The high O_3 levels are attributed to the combined effects of high-elevation surface, thermal and dynamical forcing of the Tibetan plateau and *in-situ* photochemical production in the air trapped in the plateau by surrounding mountains (Guo et al., 2015; Wang et al., 2015). The dynamic effect, associated with the large-scale circulation, is more important than the chemical effect (Tian et al., 2008; Liu et al., 2010) and responsible for the high O_3 levels over the Tibetan plateau. The six models are able to well reproduce the high surface O_3 mean concentrations (> 50 ppb) over the Tibetan plateau.

Higher O_3 mean concentrations (> 60 ppb) are also observed in Southwestern U.S., at the stations inland close to Los Angeles, in Northeastern U.S. and East Asia (e.g. Beijing) (Fig. 1). The American Southwest is an O_3 precursor hotspot where the industrial sources emit CH_4 and VOCs into the air (Jeričević et al., 2013) and the eastern and northern desert areas have higher ambient O_3 than urban areas of southern California due to four factors: on-shore winds, gasoline reformulation, eastward population expansion and nighttime air chemistry (Arbaugh and Bytnerowicz, 2003). The surface concentrations show higher O_3 levels in areas downwind of O_3 precursor sources, i.e. urban and well-industrialized areas, at distances of hundreds or even thousands of kilometers due to transport of O_3 and precursors, including "reservoir" species such as PAN, lower O_3 titration by NO and higher biogenic VOC emission (Wilson et al., 2012; Paoletti et al., 2014; Monks et al., 2015; Sicard et al., 2016a).The higher O_3 levels in areas downwind of O_3 precursor sources are well simulated in GISS-E2-R and MOCAGE models.

In the lower troposphere, O_3 can be removed by a large number of chemical reactions and by dry deposition (Sicard et al., 2016c). The O_3 dry deposition rates range from 0.01-0.05 cm s^{-1} (oceans and snow) to 0.15-1.80 cm s^{-1} for mixed wood forests (Wesely and Hicks, 2000; Zhang et al., 2003). The model performance is also related to the parameterization of the dry deposition rates.

Over Greenland, mean O_3 concentrations during the historical runs, ranged from 40 to 55 ppb (Fig. 1) except in MIROC-CHEM (20-25 ppb). Similarly, Helmig et al. (2007) reported annual mean of surface O_3 concentrations of 47 ppb over Greenland between 2000 and 2005, particularly at the high-elevation Summit station (3200 m a.s.l.). Several investigations, about snow photochemical and oxidation processes over Greenland, concluded that photochemical

O_3 production can be attributed to high levels of reactive compounds (e.g. oxidized nitrogen species) present in the surface layer during the sunlit periods due to local sources e.g. NOx enhancement from snowpack emissions, Peroxyacetyl nitrate (PAN) decomposition, boreal forest fires or ship emissions (Granier et al., 2006; Stohl et al., 2007; Legrand et al., 2009; Walker et al., 2012). PAN to NOx ratio increases with increasing altitude and latitude (Singh et al., 1992). The PAN reservoir for NOx may be responsible for the increase in surface O_3concentrations at high latitudes (Singh et al., 1992). Local O_3 production does not appear to have an important contribution to the ambient high O_3 levels (Helmig et al., 2007), however the long-range O_3 transport can elevate the background concentrations measured at remote sites, e.g. Greenland (Ellingsen et al., 2008; Derwent et al., 2010). Low dry deposition rates for O_3, the downward transport of stratospheric O_3, the photochemical local production and the large-scale transport (Legrand et al., 2009; Walker et al., 2012; Hess and Zbinden, 2013) are known factors to explain higher O_3 pollution over Greenland.

The surface O_3 concentrations (> 40 ppb) and AOT40 (> 60 ppm.h) are higher over deserts, downwind of O_3 precursor sources (e.g. Near East, Sierra Nevada, Colorado Desert), due to lower O_3 dry deposition fluxes, O_3 precursors long-range transport from urbanized areas and high insolation. Around the Mediterranean basin, elevated AOT40 values (> 60 ppm.h) are recorded, mainly due to the industrial development, road traffic increment, high insolation, sea/land breeze recirculation and O_3 transport (Sicard et al., 2013). All models, except MIROC-CHEM, are able to well reproduce the high surface O_3 mean concentrations over Greenland and over deserts.

Projected changes in ozone concentration and AOT40

Recent studies display a mean global increase in background O_3 concentration from a current level of 35-50 ppb (e.g. IPCC, 2014; Lefohn et al. 2014) to 55-65 ppb (e.g. Wittig et al., 2007) and up to 85 ppb at NH mid-latitudes by 2100 (IPCC, 2014). During the latter half of the 20th century surface O_3 concentrations have increased markedly at NH mid-latitudes (e.g. Oltmans et al., 2006; Parrish et al., 2012; Paoletti et al., 2014), mainly related to increasing anthropogenic precursor emissions related to economic growth of industrialized countries (e.g. Lamarque et al., 2005). Our results indicate that the future projections of the mean tropospheric O_3 concentrations and AOT40 vary considerably with the different scenarios and models (Fig. 1 and 2). The six models simulate a decrease of O_3 concentration by 2100 under the RCP2.6 and RCP4.5 scenarios, and an increase under the RCP8.5 scenario (Lamarque et al., 2011). In our study, the averaged relative changes in surface O_3 concentration means (and AOT40) for the different RCPs are: -21% (-75%) for RCP2.6, - 10% (-50%) for RCP4.5 and + 14% (+69%) for RCP8.5 with a strong disparity between both hemispheres, e.g. - 8% in SH and - 25% in NH for RCP2.6 (Tables 3b-c). RCP8.5 is the only scenario to show an increase in global background O_3 levels by 2100 (+ 23% in SH and + 11% in NH).

Under the RCP2.6 scenario, all models predict that tropospheric O_3 will strongly decrease worldwide, except in Equatorial Africa where higher O_3 levels are observed in GFDL-AM3, GISS-E2-R and MOCAGE. In CESM-CAM, GFDL-AM3 and MIROC-CHEM, a homogeneous decrease in O_3 burden is simulated worldwide while in GISS-E2-R, MOCAGE and UM-CAM, the strongest decrease in surface O_3 mean concentrations are found where high historical O_3 concentrations were reported. Under RCP4.5 scenario, the surface O_3 mean concentrations and AOT40 values are lower than historical runs worldwide for all models except in MOCAGE where deterioration is observed over Canada, Greenland and East Asia. For all models, the surface O_3 levels and AOT40 are higher for RCP8.5 as compared to historical runs and the highest increases occur in the Northwestern America, Greenland, Mediterranean basin, Near East and East Asia. The AOT40 values, exceeding 70 ppm.h, are found over the Tibetan plateau and in Near East and over Greenland. For RCP8.5, GFDL-AM3 is the most pessimistic model and MIROC-CHEM the most optimistic. By the end of the 21st century, similar patterns are evident for RCP4.5 compared to RCP2.6 and RCP4.5 simulation is intermediate between RCP2.6 and RCP8.5 ones.

For all models and RCPs, the O_3 hot-spots (mean concentrations > 50 ppb and AOT40 > 70 ppm.h) are over Greenland and South Asia, in particular over the Tibetan plateau. The highest increases are observed in NH, in particular in Northwestern America, Greenland, Near East and South Asia (> 65 ppb). For the three RCPs, no significant change in tropospheric O_3 is observed in SH and the SH extratropics makes a small contribution to the overall change.

A recent global study showed the geographical patterns of surface air temperature differences for late 21st century relative to the historical run (1986-2005) in all RCP scenarios (Nazarenko et al., 2015).The global warming in the RCP2.6 scenario is 2-3 times smaller than RCP4.5 scenario and 4-5 times smaller than RCP8.5 scenario (Nazarenko et al., 2015). For the three RCPs, the greatest change is observed over the Arctic, above latitude 60°N, and in the latitude band 15-45°N (IPCC, 2014; Nazarenko et al., 2015). The least warming is simulated over the large area of the Southern Ocean. For RCP8.5 scenario, the global pattern of surface O_3 levels and AOT40 (Fig. 1-2) is similar to surface air temperature increase distribution. For RCP8.5, significant increases in air temperature are simulated over latitude 60°N and over the Tibetan plateau (more than 5°C). An increase of 4-5°C over the Near East, East and South Asia, North and South Africa and Canada are simulated as well as + 1-3°C for the rest of the world (Nazarenko et al., 2015). The tropospheric warming is stronger in the latitude band 15-45°N (Seidel et al., 2008) and Hudson et al. (2006) have demonstrated that O_3 trends over a 24-year period in the NH are due to trends in the relative area of the tropics and mid-latitudes and Polar Regions.All models are able to reproduce the global pattern of air temperature changes distribution in agreement with surface O_3 concentrations changes.

The spread in precursor emissions (e.g. VOCs, NOx, CO) is due to the range of representation of biogenic emissions (NOx from soils and lightning, CO from oceans and vegetation) as well as the complexity of chemical schemes in particular for NMVOCs simulations (e.g. isoprene) from explicitly specified to fully interactive with climate. RCP2.6 scenario has the lowest O_3 precursor concentrations, and RCP8.5 has relatively low NOx, CO and VOCs emissions, but very high CH_4 (Table 2b). The global emissions of NOx (-44%), VOCs (-5%) CO (-40%) and CH_4 burden (-27%) decline, while LNOx increase by e.g. 7% under RCP2.6 (Table 2b). The CO (-32%) and NOx (-20%) emissions have decreased while LNOX (+33%), VOCS (+1%) and CH_4 burden have increased (+120%) under RCP8.5 scenario (Table 2b). The GISS-E2-R model shows a greater degree of variation than other models, with a stronger increase in CH_4 burden (+ 153%) and in VOCs emissions (+ 20%) for RCP8.5 (Table 2b).

Excluding CH_4 burden and VOCs emissions, all the RCPs include reductions and redistributions of O_3 precursor emissions throughout the 21st century, due to the air pollution control strategies worldwide. The changes in CH_4 burden are due to the different climate policies in model assumptions. In RCP2.6, CH_4 emissions decrease steadily throughout the century, in RCP4.5 it remain steady until 2050 and then decrease (Voulgarakis et al., 2013) and in RCP8.5 (no climate policy) it rapidly increase compared to 2000. Methane burdens are fixed in the models with no sources, except for the GISS-E2-R simulations in which surface CH_4 emissions are prescribed for future rather than concentrations (Shindell et al., 2012). The model chemical schemes vary greatly in their complexity, mainly due to the NMVOCs simulations (Young et al. 2013). Isoprene dominates the total NMVOCs emissions (Guenther et al., 1995). Inversely to other models with constant present-day isoprene emissions, the

GISS-ES2-R simulations incorporate climate-driven isoprene emissions, with greater BVOC emissions by 2100 and a positive change in total VOCs emissions across RCPs, related to the positive correlation between air temperature and isoprene emission (e.g. Guenther et al., 2006; Arneth et al., 2011; Young et al., 2013).

For RCP2.6 and RCP4.5 scenarios, there is a widespread decrease in O_3 in NH by 2100. The overall decrease in O_3 concentration and AOT40 means for RCP4.5 are about half of that between RCP2.6 and the historical simulation. For both scenarios, the changes are dominated by the decrease in O_3 precursor emissions in the NH extratropics compared to historical simulations (Table 2b). In NOx saturated areas, annual mean O_3 will slightly increase as a result of a less efficient titration by NO, but the overall O_3 burden will decrease substantially at hemispheric scale over time (Gao et al., 2013; Querol et al., 2014; Sicard et al., 2016a). In RCP4.5, Gao et al. (2013) showed that the largest decrease in O_3 (4-10 ppb) occurs in summer at mid-latitudes in the lower troposphere while the O_3 concentrations undergo an increase in winter. During the warm period, the photochemistry plays a major role in the O_3 production, suggesting that the reduction in surface O_3 concentrations is in agreement with the large reduction in anthropogenic O_3 precursor emissions (Sicard et al., 2016a) reducing the extent of regional photochemical O_3 formation (e.g. Derwent et al., 2013; Simpson et al., 2014). Titration effect was also reported by Collette et al. (2012) over Europe by using six chemistry transport models.

The O_3 increase can be also driven by the net impacts of climate change, i.e. increase in stratospheric O_3 intrusion, changing LNOx and impacting reaction rates, through sea surface temperatures and relative humidity changes (Lau et al., 2006; Voulgarakis et al., 2013; Young et al., 2013).

Under the RCP8.5 scenario, the increase in surface O_3 concentrations, by 14% on average, can be attributed to the higher CH_4 emissions coupled with a strong global warming, exceeding 2°C, and a weakened NO titration by reducing NOx emissions (Stevenson et al., 2013; Young et al., 2013). The global CH_4 burden are 27% and 5% lower than 2000, for the RCP2.6 and RCP4.5 scenarios respectively while for RCP8.5, the total CH_4 burden has more than doubled compared to early 2000s and LNOx emissions increased by 33% (Table 2b). In addition, stronger increases are found over the high-elevation Himalayan Plateau reflecting increased exchange with the free troposphere or stratosphere (Lefohn et al., 2012; Schnell et al., 2016).

Several studies reported an increase in the stratospheric O_3 influx and higher stratospheric O_3 levels in response to a warming climate (e.g. Hegglin and Shepherd, 2009; Zeng et al., 2010). The downwards O_3 transport from the stratosphere is an important source of tropospheric O_3 (Hsu and Prather, 2009; Tang et al., 2011), therefore, stratospheric O_3 recovery also plays a partial role (e.g. + 11% for RCP8.5) in surface O_3 burden pattern. As an example, in MOCAGE, smaller reduction in global O_3 mean concentrations (-13%) and higher increase in stratospheric O_3 inputs (+20%) are observed for RCP2.6 (Table 3b). Similarly, for RCP8.5, the highest increase in O_3 mean concentrations (+23%) and stratospheric O_3 (+24%) are recorded in MOCAGE. In addition, lightning NOx emissions show significant upward trend from 2000 to 2100, in particular for the strongest warming scenario (RPC8.5) with greater convective and lightning activity (e.g. Williams, 2009; Lamarque et al., 2013). For RCP8.5, a reduction in surface O_3 concentrations is also simulated over the equatorial region, where the increased relative humidity, in a warmer climate, increases the O_3 loss rate (e.g. Johnson et al., 1999; Zeng and Pyle, 2003).

Risk areas for vegetation under RCP scenarios

Figure 3 shows the changes in the potential O_3 injury between present and future. It should be noted that a zero percentage of change (i.e. no change) for IO3, is simulated in sparsely vegetated regions (e.g. Gobi, Sahara, Near East, Western plateau and Greenland), while the change can be higher than 100% when the historical O_3 concentrations are lower than 40 ppb (i.e. AOT40 = 0 and IO3 = 0) and the O_3 concentrations exceed 40 ppb under RCPs (i.e. AOT40 > 0, IO3 > 0).

The potential O_3 impact for vegetation strongly decreases in NH for RCP2.6, except in MOCAGE where a slight increase in the risk factor (+ 15 %) is simulated at high latitudes and in South Asia. Conversely, the areas where the risk for vegetation increases (> 60 %) occur over Africa (+ 15% to + 60%) for all models, except in CESM-CAM where no change is observed across Africa. Under RCP4.5 scenario, the strongest increase in potential risk for vegetation (> + 60 %) is simulated by MOCAGE, markedly different from the other models, above the latitude 50°N. For all models, the potential O_3 impact for vegetation increases across Africa, from - 15% to + 60% while slight decreases or no change occur worldwide. Under RCP8.5 scenario, an increase of average O_3 over a significant part of the domain is simulated, therefore the exposure to O_3 pollution and impacts on vegetation will increase worldwide by 2100. An increase of the O_3 impacts on vegetation is simulated in Northern

U.S., South America, Asia and Africa while a reduction in particular over Eastern U.S. and Southeastern China, and a slight increase (+ 15%) or decrease (- 15%) over Europe depending on the model, are simulated.

In summary, compared to the historical simulations, the averaged relative changes in the O_3 risk factor for the different RCPs are: - 61% for RCP2.6, - 47% for RCP4.5 and + 70% for RCP8.5 (Table 3d). We thus find a significant reduction in risk for vegetation for both RCP2.6 and RCP4.5 scenarios, except in South Africa and at high-latitudes in MOCAGE simulations, and a strong increase in global risk under RCP8.5. Under RCP2.6 and RCP4.5 scenarios, IO3 slightly increases in Africa and over North America and Asia (> latitude 60°N) in MOCAGE. The risk increases over the few areas where the O_3 concentrations increased between the historical period and 2100. Under both scenarios, the strongest reductions in risk are observed over Amazon, Central Africa and South Asia, i.e. where the O_3 concentrations have strongly declined between historical period and 2100. Under the RCP8.5, the areas where the highest projected O_3 mean concentrations are simulated (e.g. Greenland, deserts) are not associated to an increase in IO3 due to the absence of vegetation. Under RCP8.5, IO3 increases worldwide while a reduction is simulated over Southeast North America, northern Amazon, Central Africa and Southeast Asia, and a slighter reduction or a slight increase is simulated over Western Europe (depending on the model).

The spatial pattern of IO3 is consistent with previous analyses on climate change and O_3 impacts on vegetation (e.g. Nemani et al., 2003; Zhu et al., 2016), i.e. the highest reduction in risk for vegetation, in particular under RCP8.5, occurs over areas where a strong increase in greening, LAI and NPP is observed due to global change and where a reduction in O_3 mean concentrations is found by 2100 (Fig. 1). The regions with the largest greening trends are in Southeast North America, northern Amazon, Europe, Central Africa and Southeast Asia with an average increase of the observed LAI exceeding 0.25 $m^2\ m^{-2}$ per year (Zhu et al., 2016). The CO_2 fertilization effects (70%), nitrogen deposition (9%) and climate change (8%) explain the observed greening trend (Zhu et al., 2016). The changing climate alone produces persistent NPP increases and the regions with the highest increase in NPP, ranging from 1.0-1.5% per year, are in Southeast North America, northern Amazon, Western Europe, Central Africa and South Asia (Nemani et al., 2003). NPP increased by 6% globally between 1982 and 1999 and the highest increases are observed in tropical regions, with more than 1.5% per year over Amazon rainforest which accounts for 42% of the global NPP increase (Nemani et al., 2003). Amazon rainforest is one region where the effects are statistically significant. This is particularly important owing to the role of the Amazon rainforests in the global carbon cycle (Zhu et al., 2016). In these areas, the increasing effect of a warming climate on forests (e.g. increase of greening, LAI) is higher than the reduction in GPP due to O_3. Inversely, the risk for vegetation increases in particular in Africa, e.g. western Africa along the Gulf of Guinea, in South Brazil and over high-latitudes regions (> 60°N) in North America and Asia where a reduction or a slight increase in LAI (from - 0.05 to + 0.03 m^2 m^{-2} per year) and strong decreases, by 1.0-1.5% per year, in NPP are simulated (Nemani et al., 2003; Zhu et al., 2016).

Our results are not in agreement with the high GPP reduction, due to O_3 effects, simulated by Sitch et al. (2007) between 1901 and 2100, with a projected GPP reduction exceeding 30% over Western Europe, eastern and western North America, Amazon, central Africa and East Asia where higher surface O_3 mean concentrations were projected. Previous studies reported that the reductions in GPP simulated by Sitch et al. (2007) are overestimated up to six times (Ren et al., 2011; Zak et al., 2011; Kvaleveg and Myhre 2013), mainly due to the lack of empirical data about the response of different species to O_3, the fact that a few experiments have shown no response, e.g. grasslands (Bassin et al., 2013), and the non-inclusion of the nitrogen limitation of growth (Kvalevag and Myhre, 2013).

The projected land covers widely vary under RCPs (Betts et al., 2015). In RCP2.6 scenario, the ground surface covered by croplands increases as a result of bio-energy production, with a more-or-less constant use of grassland. The RCP4.5 scenario focuses on global reforestation programs as part of global climate policy, as a result, the use of cropland and grassland decreases. Under RCP8.5, an increase in croplands and grasslands is applied mostly driven by an increasing global population (van Vuuren et al., 2011). Generally, the risk for vegetation strongly increases over shrublands (e.g. high-latitude region, Australia, South Africa) and savannas (e.g. South Brazil, Africa) and the risk decreases over forests, strongly over evergreen broadleaf forest and deciduous woodland over Africa and Amazon rainforests, and slighter over needleleaf forests in Northern America (Canada) and Northern Asia. The risk slightly decreases or slightly increases over grasslands (Central Asia and central Africa and U.S.). The largest decreases (50-80%) under RCP8.5 occur in Eastern U.S., Europe and Southeastern China, where the ground is mainly dominated by croplands, in all models except CESM-CAM.

Conclusions

From six global atmospheric chemistry transport models, we illustrate the changes, i.e. differences for late 21st century relative to the historical run, in ground-level O_3 concentrations and vegetation impact metric (AOT40). *In fine*, the potential O_3 impacts on vegetation worldwide are investigated to define potential risk areas for vegetation at global scale by 2100.

The six models are able to well reproduce the spatial pattern of historical O_3 concentration and AOT40 at global scale, in particular GISS-E2-R and MOCAGE are able to simulate the higher O_3 levels in areas downwind of precursor sources and at the high-elevation areas. The model outputs emphasize the strong asymmetry in the tropospheric O_3 distribution between NH and SH; substantially higher O_3 mean concentrations are observed in the NH (ca. 38 ppb), particularly in the latitude band 15-45°N, than in the SH (ca. 23 ppb). The natural emissions of O_3 precursors (e.g. lightning NOx, CO from oceans, isoprene) as well as the complexity of chemical schemes are significant sources of model-to-model differences.

In this study, the projected mean tropospheric O_3 concentrations and AOT40 dependent on global and regional emission pathways. Compared to early 2000s, the results suggest changes in surface O_3 of - 9.5 ± 2.0 ppb (NH) and - 1.8 ± 2.1 ppb (SH) in the cleaner RCP2.6 scenario and of + 4.4 ± 2.8 ppb (NH) and + 5.1 ± 2.1 ppb (SH) in RCP8.5 scenario. For RCP2.6 and RCP4.5, absolute decreases are observed for the Mediterranean basin and the Western U.S. due to less precursor emissions in the NH extratropics (e.g. reduction of 5-7 ppb over Europe). Smaller reduction in surface O_3 levels in South and East Asia highlight the smaller changes in O_3 precursor emissions due to the recent emission growth in this region (e.g. Zhang et al., 2009; Xing et al., 2015). For RCP8.5, all models show climate-driven increases in ground-level O_3 in particular over the Western U.S, Greenland, South Asia and Northeast China. The changes in surface O_3 over North America and Europe ranged from + 1-5 ppb under RCP8.5. South Asia sees the greatest increase, up to more than 10 ppb for RCP 8.5. The O_3 increase can be attributed to substantial increase in CH_4 emissions coupled with a strong global warming, exceeding 2°C, and a weakened NO titration and a greater stratospheric O_3 influx (Kawase et al., 2011; Wild et al., 2012; Young et al., 2013). A decline in CH_4 emissions will undoubtedly benefit future O_3 control.

The current surface O_3 levels (35-50 ppb in NH) are high enough to damage both forests and crops. About 50% of forests, grasslands and croplands might be exposed to high O_3 levels by the end of the 21st century (Sitch et al., 2007; Wittig et al. 2009). Most important results from the study are the significant overrun of exposure metric (AOT40) in comparison with the AOT40-based critical level for the protection of forests (5 ppm.h) and crops (3 ppm.h). The global models suggest that exposure-based critical levels will be exceeded over many areas of the NH, and in parts of North America, East and South Asia they may be exceeded by a factor exceeding 10 under RCP8.5. The critical level were defined for boreal and temperate deciduous tree species, i.e. more consistent for regions in the latitude band 35-60°N. To protect vegetation, the current AOT40 index appears inadequate for a realistic quantification of O_3 impacts on vegetation (Paoletti and Manning, 2007; Mills et al., 2011; De Marco et al., 2015; Sicard et al., 2016b,c). As a result, in the last decade, the United Nations Convention on Long-Range Transboundary Air Pollution (CLRTAP) has introduced the flux-based metric for vegetation protection against effects of O_3, taking into account the modifying effects of multiple climatic and phenological factors on O_3 uptake (Paoletti and Manning, 2007; Sicard et al., 2016b,c).

Ozone may be a major threat to biodiversity over large regions of the world (Sicard et al., 2016b), however the size of these areas remains uncertain. The potential O_3 impact on assimilation, IO3, provides a clear indicator of the potential risk to vegetation. The risk for vegetation decreases by about 61% and 47% under RCP2.6 and RCP4.5, respectively and increases by 70% under RCP8.5, compared to early 2000s over the whole domain by 2100 and that the potential risk areas for vegetation vary worldwide according to the dominant vegetation cover. The strongest increase of the O_3 impacts on vegetation is simulated in Northern America and Asia and central Africa. The highest reduction in risk for vegetation (i.e. Southeast North America, the northern Amazon, Central Africa and Southeast Asia) occurs over areas where a strong increase in greening, LAI and NPP is observed and where a reduction in O_3 mean concentrations is found by 2100.

Trees possess a defence capacity, e.g. through antioxidant activity and a capacity of repairing injured tissues (Paoletti, 2007).The short-term response to O_3 is a reduction in productivity of crops and forests and long-term changes in community composition could be observed due to species-specific O_3-sensitivity (Wittig et al., 2009). Generally, deciduous woodland are highly O_3-sensitive risk areas, grasslands and needleleaf forests are moderately O_3-sensitive risk

Atmos. Chem. Phys. Discuss., doi:10.5194/acp-2017-74, 2017
Manuscript under review for journal Atmos. Chem. Phys.
Discussion started: 9 March 2017

areas while the lower risk areas include evergreen broadleaf forests . However, crops are more sensitive to O_3 exposure than trees and deciduous trees are more sensitive than coniferous trees with lower stomatal conductance (Felzer et al., 2004; Ren et al., 2007; Wittig et al. 2009; Anav et al., 2011). To efficiently protect vegetation against O_3 pollution, suitable standards taking into account the detoxification processes (e.g. flux-based metric) are urgently needed.

As the vegetation atmosphere feedbacks are still under investigated, e.g. impacts of changes of vegetation on air chemistry, we recommend the use of improved chemistry-climate modelling system, fully coupled with dynamic vegetation models, to perform high resolution simulations and to better evaluate the regional exposure of ecosystems to air pollution.

The risk reduction is possible through climate-change mitigation, e.g. reductions in air pollution, and adaptation actions. An efficient reduction in overall O_3 levels is expected over North America and Europe in all RCP scenarios and worldwide if CH_4 emissions are reduced (e.g. Kirtman et al., 2013; Pfister et al., 2014; Schnell et al., 2016). However, the increasing effect of a warming climate on surface O_3 concentrations is higher than the reduction achieved by the decline in O_3 precursor emissions (Revell et al., 2015; Hendriks et al., 2016), therefore, climate change and the measures and policies in e.g. Asia will need to be factored into future O_3 policies (Wilson et al., 2012; Lefohn and Cooper, 2015). Many ecosystems worldwide are unprotected from O_3 due to the lack of international efforts (Emberson et al., 2014). To be efficient, the mitigation actions for O_3 impacts on biodiversity must be as part of international emission reduction programmes.

Acknowledgements

This work was carried out with the contribution of the LIFE financial instrument of the European Union (LIFE15 ENV/IT/183) in the framework of the MOTTLES project "Monitoring ozone injury for setting new critical levels" and published within the International Union of Forest Research Organizations (IUFRO) Task Force on Climate Change and Forest Health.

Bibliographic references

Ainsworth E.A., Yendrek C.R., Sitch S., Collins, W.J., Emberson L.D., 2012, "The effect of Tropospheric Ozone on Net Primary Productivity and Implications for Climate Change". Annu. Rev. Plant Biol. 63: 637-661

Anav A., Menut L., Khvorostyanov D., Viovy N., 2011, "Impact of tropospheric ozone on the Euro-Mediterranean vegetation". Global Change Biol. 17: 2342-2359

ArbaughM.J., and Bytnerowicz A., 2003, "Ambient ozone patterns and effects over the Sierra Nevada: synthesis and implications for future research". In: A. Bytnerowicz, M. Arbaugh, R. Alonso (eds), Ozone Air Pollution in the Sierra Nevada: Distribution and Effects on Forests, Developments in Environmental Science, vol. 2, Elsevier, Amsterdam, 249-261

Arneth A., Schurgers G., Lathière J., Duhl T., Beerling D. J., et al., 2011, "Global terrestrial isoprene emission models: sensitivity to variability in climate and vegetation". Atmos. Chem. Phys. 11: 8037-8052

Arneth A., Schurgers G., Hickler T., Miller P.A., 2008, "Effects of species composition, land surface cover, CO_2 concentration and climate on isoprene emissions from European forests". Plant Biol. 10: 150-162

Ashmore M.R., 2005, "Assessing the future global impacts of ozone on vegetation". Plant Cell Environ. 28: 949-964

Ashworth K., Wild O., Hewitt C.N., 2013, "Impacts of biofuel cultivation on mortality and crop yields". Nat. Clim. Change 3: 492-496

Bassin S., Volk M., Fuhrer J., 2013, "Species composition of subalpine grassland is sensitive to nitrogen deposition, but not ozone, after seven years of treatment". Ecosystems 16: 1105-1117

Betts R.A., Golding N., Gonzalez P., Gornall J., Kahana R., et al., 2015, "Climate and land use change impacts on global terrestrial ecosystems and river flows in the HadGEM2-ES Earth system model using the representative concentration pathways". Biogeosciences 12: 1317-1338

Bian J., Yan R., Chen H., Lü D., Massie S.T., 2011, "Formation of the summertime ozone valley over the Tibetan Plateau: The Asian summer monsoon and air column variations". Adv. Atmos. Sci. 28: 1318-1325

Bowman K.W., Shindell D.T., Worden H.M., Lamarque J.F., Young P.J., 2013, "Evaluation of ACCMIP outgoing longwave radiation from tropospheric ozone using TES satellite observations". Atmos. Chem. Phys. 13: 4057-4072

Clifton O.E., Fiore A.M., Correa G., Horowitz L.W., Naik V., 2014, "Twenty-first century reversal of the surface ozone seasonal cycle over the northeastern United States". Geophys. Res. Lett. 41: 7343-7350

Chen X.L., Ma Y.M., Kelder H., Su Z., Yang K., 2011, "On the behaviour of the tropopause folding events over the Tibetan Plateau". Atmos. Chem. Phys. 11: 5113-5122

Chevalier A., Gheusi F., Delmas R., Ordóñez C., Sarrat C., et al., 2007, "Influence of altitude on ozone levels and variability in the lower troposphere: a ground-based study for Western Europe over the period 2001-2004". Atmos. Chem. Phys. 7: 4311-4326

Colette A., Granier C., Hodnebrog Ø., Jakobs H., Maurizi A., et al., 2012, "Future air quality in Europe: a multi-model assessment of projected exposure to ozone". Atmos. Chem. Phys. 12: 10613-10630

Cooper O.R., Parrish D.D., Ziemke J., Balashov N.V., Cupeiro M., 2014, "Global distribution and trends of tropospheric ozone: An observation-based review". Elementa: Science of the Anthropocene 2: 000029

Cooper O.R., Sweeney C., Gao R.S., Tarasick D., Leblanc T., 2012, "Long-term ozone trends at rural ozone monitoring sites across the United States, 1990-2010". J. Geophys. Res. 117: D22307

Cubasch U., Wuebbles D., Chen D., Facchini M.C., Frame D., et al., 2013, "Introduction, in Climate Change 2013: The Physical Science Basis". Contribution of Working Group I to the Fifth Assessment Report of the Intergovernmental Panel on Climate Change, edited by T. F. Stocker et al., Cambridge Univ. Press, Cambridge, U. K. and New York

De Marco A., Sicard P., Vitale M., Carriero G., Renou C., et al., 2015, "Metrics of ozone risk assessment for Southern European forests: canopy moisture content as a potential plant response indicator". Atmos. Environ. 120: 182-190

Derwent R.G., Utembe S.R., Jenkin M.E., Shallcross D.E., 2015, "Tropospheric ozone production regions and the intercontinental origins of surface ozone over Europe".Atmos. Environ. 112: 216-224

Derwent R.G., Manning A.J., Simmonds P.G., Spain T.G., O'Doherty S., 2013, "Analysis and interpretation of 25 years of ozone observations at the Mace Head Atmospheric Research Station on the Atlantic Ocean coast of Ireland from 1987 to 2012". Atmos. Environ. 80: 361-368

Derwent R.G., Witham C.S., Utembe S.R., Jenkin M.E., Passant N.R., 2010, "Ozone in Central England: the impact of 20 years of precursor emission controls in Europe". Environ. Sci. Policy 13: 195-204

Donner L.J., Wyman B.L., Hemler R.S., Horowitz L.W., Ming Y., et al., 2011, "The dynamical core, physical parameterizations, and basic simulation characteristics of the atmospheric component AM3 of the GFDL Global Coupled Model CM3". J. Climate 24: 3484-3519

European Environment Agency, 2015 "Air quality in Europe - 2015 report".ISBN 978-92-9213-702-1. Report No 5/2015

Ellingsen K., Gauss M., Van Dingenen R., Dentener F.J., Emberson L., et al., 2008, "Global ozone and air quality: a multi-model assessment of risks to human health and crops". Atmos. Chem. Phys. 8: 2163-2223

Emberson L.D., Fuhrer J., Ainsworth L., Ashmore M.R., 2014, "Biodiversity and Ground-level Ozone". Report UNEP/CBD/SBSTTA/18/INF/17. Convention on Biological Diversity, 18th meeting, Montreal, 23-28 June 2014

Fares S., Vargas R., Detto M., Goldstein A.H., Karlik J., et al., 2013, "Tropospheric ozone reduces carbon assimilation in trees: estimates from analysis of continuous flux measurements". Global Change Biol.19: 2427-2443

Federal Register, 2015, "National Ambient Air Quality Standards for Ozone". 40 CFR Part 50, 51, 52, 53, and 58, pp 65292-65468

Felzer B.S.F., Kicklighter D.W., Melillo J.M., Wang C., Zhuan Q., et al., 2004, "Ozone effects on net primary production and carbon sequestration in the conterminous United States using a biogeochemistry model". Tellus B 56: 230-248

Fiore A.M., Naik V., Leibensperger E.M., 2015, "Air quality and climate connections". J. Air Waste Manage. Assoc. 65: 645-685

Fiore A.M., Naik V.,Spracklen D.V., Steiner A., Unger N. et al., 2012, "Global air quality and climate". Chem. Soc. Rev. 41: 6663-6683

Fiscus E.L., Booker F.L., Burkey K.O., 2005, "Crop responses to ozone: uptake, modes of action, carbon assimilation and partitioning". Plant Cell Environ. 28: 997-1011

Gao Y., Fu J.S., Drake J.B., Lamarque J.F., Liu Y., 2013, "The impact of emission and climate change on ozone in the United States under representative concentration pathways (RCPs)". Atmos. Chem. Phys. 13: 9607-9621

Granier C., Niemeier U., Jungclaus J.H., Emmons L., Hess P., et al., 2006, "Ozone pollution from future ship traffic in the Arctic northern passages". Geophys. Res. Lett. 33, doi: 10.1029/2006GL026180

Guenther A.B., Karl T., Harley P., Wiedinmyer C., Palmer P.I., Geron C., 2006, "Estimates of global terrestrial isoprene emissions using MEGAN (Model of Emissions of Gases and Aerosols from Nature)". Atmos. Chem. Phys. 6: 3181-3210

Guenther A.B., Hewitt C.N., Erickson D., Fall R., Geron, C., et al., 1995, "A global model of natural volatile organic compound emissions". J. Geophys. Res. 100: 8873-8892

Guo D., Su Y., Shi C., Xunn J., Powell Jr. A.M., 2015, "Double core of ozone valley over the Tibetan Plateau and its possible mechanisms". Journal of Atmospheric and Solar-Terrestrial Physics 130: 127-131

Hegglin M.I. and Shepherd T.G., 2009, "Large climate-induced changes in ultraviolet index and stratosphere-to-troposphere ozone flux". Nature Geosci. 2: 687

Helmig D., Oltmans S.J., Morse T.O., Dibb J.E., 2007, "What is causing high ozone at Summit, Greenland?". Atmos. Environ. 41: 5031-5043

Hendriks C., Forsell N., Kiesewetter G., Schaap M., Schöpp W., 2016, "Ozone concentrations and damage for realistic future European climate and air quality scenarios". Atmos. Environ. 144: 208-219

Hess P.G. and Zbinden R., 2013, "Stratospheric impact on tropospheric ozone variability and trends: 1990-2009". Atmos. Chem. Phys. 13: 649-674

Holland M., Kinghorn S., Emberson L., Cinderby S., Ashmore M., et al., 2006, "Development of a framework for probabilistic assessment of the economic losses caused by ozone damage to crops in Europe". UNECE International Cooperative Programme on Vegetation. Contract Report EPG 1/3/205. CEH Project No: C02309NEW

Hsu J. and Prather M.J., 2009, "Stratospheric variability and tropospheric ozone". J. Geophys. Res. 114: D06102

Hu X.M, Klein Petra M., Xue M. et al., 2013, "Impact of the vertical mixing induced by low-level jets on boundary layer ozone concentration". Atmos. Environ. 70: 123-130

Hudson R.D., Andrade M.F., Follette M.B., Frolov A.D., 2006, "The total ozone field separated into meteorological regimes – Part II: Northern Hemisphere mid-latitude total ozone trends". Atmos. Chem. Phys. 6: 5183-5191

IPCC, Intergovernmental Panel on Climate Change, 2014, "Summary for Policymakers". In: "Climate Change 2014: Impacts, Adaptation and Vulnerability". Contribution of Working Group II to the Fifth Assessment Report of the Intergovernmental Panel on Climate Change. Cambridge University Press, Cambridge, UK

Jeričević A., Koračin D., Jiang J., Chow J., Watson J., et al., 2013, "Air Quality Study of High Ozone Levels in South California". Part of the series NATO Science for Peace and Security Series C: Environmental Security. Air Pollution Modeling and its Application XXII: 629-633

Johnson C.E., Collins W.J., Stevenson D.S., Derwent R.G., 1999, "Relative roles of climate and emissions changes on future tropospheric oxidant concentrations". J. Geophys. Res. 104: 18631-18645

Josse B., Simon P., Peuch V.H., 2004, "Radon global simulations with the multiscale chemistry and transport model MOCAGE". Tellus-B 56: 339-356

Kawase H., Nagashima T., Sudo K., Nozawa T., 2011, "Future changes in tropospheric ozone under Representative Concentration Pathways (RCPs)". Geophys. Res. Lett. 38: L05801

Kelly J., Makar P.A., Plummer D.A., 2012, "Projections of mid-century summer air-quality for North America: effects of changes in climate and precursor emissions". Atmos. Chem. Phys. 12: 5367-5390

Kirtman B., Power S.B., Adedoyin J.A., Boer G.J., Bojariu R., et al., 2013, "Near-term climate change: Projections and predictability, in Climate Change 2013: The Physical Science Basis". Contribution of Working Group I to the Fifth Assessment Report of the

Atmos. Chem. Phys. Discuss., doi:10.5194/acp-2017-74, 2017
Manuscript under review for journal Atmos. Chem. Phys.
Discussion started: 9 March 2017

Atmospheric Chemistry and Physics Discussions

Intergovernmental Panel on Climate Change, edited by T.F. Stocker et al., Cambridge Univ. Press, Cambridge, U. K., and New York

Klingberg J., Engardt M., Karlsson P.E., Langner J., Pleijel H., 2014, "Declining ozone exposure of European vegetation under climate change and reduced precursor emissions". Biogeosciences 11: 5269-5283

Krinner G., Viovy N., de Noblet-Ducoudré N., Ogée J., Polcher J., et al., 2005, "A dynamic global vegetation model for studies of the coupled atmosphere-biosphere system". Global Biogeochem. Cy. 19: GB1015

Kulkarni P.S., Bortoli D., Domingues A., Silva A.M., 2015, "Surface Ozone Variability and Trend over Urban and Suburban Sites in Portugal". Aerosol Air Qual. Res.: 1-15

Kulkarni P.S., Bortoli D., Salgado R., Anton M., Costa M.J., et al., 2011, "Tropospheric ozone variability over the Iberian Peninsula". Atmos. Environ. 45: 174-182

Kvalevag M.M. and Myrhe G., 2013, "The effect of carbon-nitrogen coupling on the reduced land carbon sink caused by ozone". Geophys. Res. Lett. 40: 3227-3231

Lamarque J.F., Shindell D.T., Josse B., Young P.J., Cionni I., et al., 2013, "The Atmospheric Chemistry and Climate Model Intercomparison Project (ACCMIP): overview and description of models, simulations and climate diagnostics". Geosci. Model Dev. 6: 179-206

Lamarque J.F., Emmons L.K., Hess P.G., Kinnison D.E., Tilmes, S., et al., 2012, "CAM-chem: description and evaluation of interactive atmospheric chemistry in the Community Earth System Model". Geosci. Model Dev. 5: 369-411

Lamarque J.F., Bond T.C., Eyring V., Granier C., Heil A., et al., 2010, "Historical (1850–2000) gridded anthropogenic and biomass burning emissions of reactive gases and aerosols: methodology and application". Atmos. Chem. Phys. 10: 7017-7039

Lamarque J.F., Hess P.G., Emmons L.K., Buja L.E., Washington W.M., Granier C., 2005, "Tropospheric ozone evolution between 1890 and 1990". J. Geophys. Res. 110: D08304

Langner J., Engardt M., Baklanov A., Christensen J.H., Gauss M., et al., 2012, "A multi-model study of impacts of climate change on surface ozone in Europe". Atmos. Chem. Phys. 12: 10423-10440

Lau N.C., Leetmaa A., Nath M.J., 2006, "Attribution of atmospheric variations in the 1997-2003 period to SST anomalies in the Pacific and Indian Ocean basins". J. Climate 19: 3607-3628

Lee Y.H.and Adams P.J., 2011, "A fast and efficient version of the two-moment aerosol sectional (TOMAS) global aerosol microphysics model". Aerosol Sci. Tech. 46: 678-689

Lefohn A.S., Malley C.S., Simon H., Wells B., Xu X., et al., 2017, "Responses of human health and vegetation exposure metrics to changes in ozone concentration distributions in the European Union, United States, and China". Atmos. Environ. 152: 123-145

Lefohn A.S. and Cooper O.R, 2015, "Introduction to the Special Issue on Observations and Source Attribution of Ozone in Rural Regions of the Western United States". Atmos. Environ. 109: 279-281.

Lefohn A.S., Emery C., Shadwick D., Wernli H., Jung J., OltmansS.J.,2014, "Estimates of background surface ozone concentrations in the United States based on model-derived source apportionment". Atmos. Environ. 84:275-288.

Lefohn A.S., Wernli H., Shadwick D., Oltmans S.J., Shapiro M., 2012, "Quantifying the frequency of stratospheric-tropospheric transport affecting enhanced surface ozone concentrations at high- and low-elevation monitoring sites in the United States". Atmos. Environ. 62: 646-656

Lefohn A.S., Shadwick D., Oltmans S.J., 2010, "Characterizing changes in surface ozone levels in metropolitan and rural areas in the United States for 1980-2008 and 1994-2008". Atmos. Environ. 44: 5199-5210

Atmospheric Chemistry and Physics
Discussions
Open Access

Legrand M.,Preunkert S., Jourdain B., Gallée H., Goutail F., et al., 2009, "Year-round record of surface ozone at coastal (Dumont d'Urville) and inland (Concordia) sites in East Antarctica". J. Geophys. Res. 114: doi: 10.1029/2008JD011667

Liu C., Liu Y., Cai Z., Gao S., Bian J., et al., 2010, "Dynamic formation of extreme ozone minimum events over the Tibetan Plateau during northern winters 1987-2001". J. Geophys. Res. 115: D18311

Meinshausen M., Wigley T.M.L., Raper S.C.B., 2011, "Emulating atmosphere-ocean and carbon cycle models with a simpler model, MAGICC6 - Part 2: Applications". Atmos. Chem. Phys. 11: 1457-1471

Mills G., Hayes F., Simpson D., Emberson L., Norris D., et al., 2011, "Evidence of widespread effects of ozone on crops and (semi-)natural vegetation in Europe (1990-2006) in relation to AOT40 and flux-based risk maps". Global Change Biol. 17: 592-613

Monks P.S., Archibald A.T., Colette A., Cooper O., Coyle M., et al., 2015, "Tropospheric ozone and its precursors from the urban to the global scale from air quality to short-lived climate forcer". Atmos. Chem. Phys. 15: 8889-8973

Myhre G., Shindell D., Bréon F.M., Collins W., Fuglestvedt J., et al., 2013, "Anthropogenic and Natural Radiative Forcing". In: Climate Change 2013: The Physical Science Basis. Contribution of Working Group I to the Fifth Assessment Report of the Intergovernmental Panel on Climate Change. Cambridge University Press, Cambridge, United Kingdom and New York, USA

Naik V., Voulgarakis A., Fiore A.M., Horowitz L.W., Lamarque J.F., et al., 2012, "Preindustrial to present day changes in tropospheric hydroxyl radical and methane lifetime from the Atmospheric Chemistry and Climate Model Intercomparison Project (ACCMIP)". Atmos. Chem. Phys. Discuss. 12: 30755-30804

Nazarenko L., Schmidt G.A., Miller R.L., Tausnev N., Kelley M., et al., 2015, "Future climate change under RCP emission scenarios with GISS ModelE2". J. Adv. Model. Earth Syst. 7: 244-267

Nemani R.R., Keeling C.D., Hashimoto H., Jolly W.M., Piper S.C., et al., 2003, "Climate-Driven Increases in Global Terrestrial Net Primary Production from 1982 to 1999".Science 300: 1560-1563

Ollinger S.V., Aber J.D., Reich P.B., 1997, "Simulating ozone effects on forest productivity: interactions among leaf, canopy, and stand-level processes". Ecol. Appl. 7: 1237-1251.

Oltmans S.J., Lefohn A.S., Harris J.M., Galbally I., Scheel H.E., et al., 2006, "Long-term changes in tropospheric ozone". Atmos. Environ. 40: 3156-3173

Paoletti E., De Marco A., Beddows D.C.S., Harrison R.M., Manning W.J., 2014, "Ozone levels in European and USA cities are increasing more than at rural sites, while peak values are decreasing". Environ. Pollut. 192: 295-299

Paoletti E., Contran N., Bernasconi P., Günthardt-Goerg M.S., Vollenweider P., 2009, "Structural and physiological responses to ozone in Manna ash (*Fraxinus ornus L.*) leaves in seedlings and mature trees under controlled and ambient conditions". Sci. Total Environ. 407: 1631-1643

Paoletti E. and Manning W.J., 2007, "Toward a biologically significant and usable standard for ozone that will also protect plants". Environ. Pollut. 150: 85-95

Paoletti E., 2006, "Impact of ozone on Mediterranean forest: A review". Environ. Pollut. 144: 463-474

Parrish D.D., Law K.S., Staehelin J., Derwent R., Cooper O.R., et al., 2012, "Long-term changes in lower tropospheric baseline ozone concentrations at northern mid-latitudes". Atmos. Chem. Phys. 12: 11485-11504

Pfister G.G., Walters S., Lamarque J.F., Fast J., Barth M.C., et al., 2014, "Projections of future summertime ozone over the U.S". J. Geophys. Res. Atmos. 119: 5559-5582

Price C. and Rind D.H., 1992, "A simple lightning parameterization for calculating global lightning distributions". J. Geophys. Res., 97: 9919-9933

Proietti C., Anav A., De Marco A., Sicard P., Vitale M., 2016, "A multi-sites analysis on the ozone effects on Gross Primary Production of European forests". Sci. Total Environ. 556: 1-11

Querol X., Alastuey A., Pandolfi M., Reche C., Pérez N., et al., 2014, "2001-2012 trends on air quality in Spain". Sci. Total Environ. 490: 957-969.

Reich P.B., 1987, "Quantifying plant response to ozone: a unifying theory". Tree Physiol. 3: 63-91

Ren W., Tian H., Liu M., Zhang C., Chen G., et al., 2007,"Effects of tropospheric ozone pollution on net primary productivity and carbon storage in terrestrial ecosystems of China". J. Geophys. Res. 112: 1-17

Revell L.E., Tummon F., Stenke A., Sukhodolov T., Coulon A., et al., 2015,"Drivers of the tropospheric ozone budget throughout the 21stcentury under the medium-high climate scenario RCP 6.0". Atmos. Chem. Phys. 15: 5887-5902

Riahi K., Rao S., Krey V., Cho C., Chirkov V., et al., 2011, "RCP 8.5 - A scenario of comparatively high greenhouse gas emissions". Climatic Change 109: 33-57

Rieder H.E., Fiore A.M., Horowitz L.W., Naik V., 2015, "Projecting policy-relevant metrics for high summertime ozone pollution events over the eastern United States due to climate and emission changes during the 21stcentury". J. Geophys. Res. Atmos. 120: 784-800

Ridley B.A., Pickering K.E., Dye, J.E., 2005, "Comments on the parameterization of lightning-produced NO in global chemistry-transport models". Atmos. Environ. 39: 6184-6187

Sanderson M.G., Collins W.J., Hemming D.L., Betts R.A., 2007, "Stomatal conductance changes due to increasing carbon dioxide levels: Projected impact on surface ozone levels". Tellus 59B: 404-411

Sanderson M.G., Jones C.D., Collins W.J., Johnson C.E., Derwent R.G., 2003, "Effect of climate change on isoprene emissions and surface ozone levels". Geophys. Res. Lett. 30: 1936

Schnell J.L., Prather M.J., Josse B., Naik V., Horowitz L.W., et al., 2016, "Effect of climate change on surface ozone over North America, Europe, and East Asia". Geophys. Res. Lett.43: L068060

Seidel D.J., Fu Q., Randel W.J., Reichler T.J., 2008, "Widening of the tropical belt in a changing climate". Nat. Geosci 1: 21-4

Shindell D.T., Lamarque J.F., Schulz M., Flanner M., Jiao C., et al., 2012, "Radiative forcing in the ACCMIP historical and future climate simulations".Atmos. Chem. Phys. Discuss. 12: 21105-21210

Shindell D.T., Faluvegi G., Stevenson D.S., Krol M.C., Emmons L.K., et al., 2006, "Multi-model simulations of carbon monoxide: Comparison with observations and projected near-future changes". J. Geophys. Res. 111: D19306

Sicard P., Serra R., Rossello P., 2016a, "Spatiotemporal trends of surface ozone concentrations and metrics in France". Environ. Res. 149: 122-144

Sicard P, Augustaitis A., Belyazid S., Calfapietra C., De Marco A., et al., 2016b, "Global topics and novel approaches in the study of air pollution, climate change and forest ecosystems". Environ. Pollut.213: 977-987

Sicard P., De Marco A., Dalstein-Richier L., Tagliaferro F., Paoletti E., 2016c, "An epidemiological assessment of stomatal ozone flux-based critical levels for visible ozone injury in Southern European forests". Sci. Total Environ. 541: 729-741

Sicard P., De Marco A., Troussier F., Renou C., Vas N., Paoletti E., 2013, "Decrease in surface ozone concentrations at Mediterranean remote sites and increase in the cities". Atmos. Environ. 79: 705-715

Sicard P., Vas N., Dalstein-Richier L., 2011, "Annual and seasonal trends for ambient ozone concentration and its Impact on Forest Vegetation in Mercantour National Park (South-eastern France) over the 2000-2008 period". Environ. Pollut. 159: 351-362

Sicard P., Coddeville P., Galloo J.C., 2009, "Near-surface ozone levels and trends at rural stations in France over the 1995-2003 period". Environ. Monit. Assess. 156: 141-157

Simpson D., Arneth A., Mills G., Solberg S., Uddling J., 2014, "Ozone - the persistent menace: interactions with the N cycle and climate change". Curr. Opin. Env. Sust. 9-10: 9-19

Singh H.B., Herlth D., O'Hara D., Zahnle K., Bradshaw J.D., et al., 1992, "Relationship of Peroxyacetyl nitrate to active and total odd nitrogen at northern high latitudes: influence of reservoir species on NOx and O_3". J. Geophys. Res. 97:16523-30

SitchS., Cox P.M., Collins W.J., Huntingford C., 2007, "Indirect radiative forcing of climate change through ozone effects on the land-carbon sink". Nature 448: 791-794

Steinbacher M., Henne S., Dommen J., Wiesen P., Prevot A.S.H., 2004, "Nocturnal trans-alpine transport of ozone and its effects on air quality on the Swiss Plateau". Atmos. Environ. 38: 4539-4550

Stevenson D.S., Young P.J., Naik V., Lamarque J.F., Shindell D.T., et al., 2013, "Tropospheric ozone changes, radiative forcing and attribution to emissions in the Atmospheric Chemistry and Climate Model Inter-comparison Project (ACCMIP)". Atmos. Chem. Phys. 13: 3063-3085

Stevenson D.S., Young P.J., Naik V., Lamarque J.F., Shindell D.T., et al., 2012, "Tropospheric ozone changes, radiative forcing and attribution to emissions in the Atmospheric Chemistry and Climate Model Inter-comparison Project (ACCMIP)". Atmos. Chem. Phys. Discuss. 12: 26047-26097

Stevenson D.S., Dentener F.J., Schultz M.G., Ellingsen K., van Noije T.P.C., et al., 2006, "Multi-model ensemble simulations of present-day and near-future tropospheric ozone". J. Geophys. Res. 111: D08301

Stevenson D.S., Johnson C.E., Collins W.J., Derwent R.G., Edwards J.M., 2000, "Future estimates of tropospheric ozone radiative forcing and methane turnover – The impact of climate change". Geophys. Res. Lett. 27: 2073-2076

Stohl A., Berg T., Burkhart J.F., Fjaeraa A.M., Forster C., et al., 2007, « Arctic smoke - record high air pollution levels in the European Arctic due to agricultural fires in Eastern Europe in spring 2006".Atmos. Chem. Phys. 7: 511-534

Tang Q., Prather M.J., Hsu J., 2011, "Stratosphere-troposphere exchange ozone flux related to deep convection". Geophys. Res. Lett. 38: L03806

Teyssèdre H., Michou M., Clark H.L., Josse B., Karcher F., et al., 2007, "A new tropospheric and stratospheric Chemistry and Transport Model MOCAGE-Climat for multi-year studies: evaluation of the present-day climatology and sensitivity to surface processes". Atmos. Chem. Phys. 7: 5815-5860

Tian W., Chipperfield M., Huang Q., 2008, "Effects of the Tibetan Plateau on total column ozone distribution". Tellus 60B: 622-635

UNECE, United Nations Economic Commission for Europe. Convention on Long-Range Trans-boundary Air Pollution, 2010, "Mapping Critical Levels for Vegetation". nternational Cooperative Programme on Effects of Air Pollution on Natural Vegetation and Crops, Bangor, UK

van Vuuren D., Edmonds J., Kainuma M., Riahi K., Thomson A., et al., 2011, "The representative concentration pathways: an overview". Climatic Change 109: 5-31

Voulgarakis A., Naik V., Lamarque J.F., Shindell D.T., Young P.J. et al., 2013, "Analysis of present day and future OH and methane lifetime in the ACCMIP simulations". Atmos. Chem. Phys. 13: 2563-2587

Walker T.W.,Jones D.B.A., Parrington M., Henze D.K., Murray L.T., et al., 2012, "Impacts of mid-latitude precursor emissions and local photochemistry on ozone abundances in the Arctic". Journal of Geophysical Research: Atmospheres 117, doi: 10.1029/2011JD016370

Wang Q.Y., Gao R.S., Cao J.J., Schwarz J.P., Fahey D.W., et al. 2015, "Observations of high level of ozone at Qinghai Lake basin in the northeastern Qinghai-Tibetan Plateau, western China". J. Atm. Chem. 72: 19-26

Wang X.and Mauzerall D.L., 2004, "Characterizing distributions of surface ozone and its impact on grain production in China, Japan and South Korea: 1900 and 2020". Atmos. Environ. 38: 4383-4402

Watanabe S., Hajima T., Sudo K., Nagashima T., Takemura T., et al., 2011, "MIROC-ESM 2010: model description and basic results of CMIP5-20c3m experiments". Geosci. Model Dev. 4: 845-872

Wesely M.L. and Hicks B.B., 2000, "A review of the current status of knowledge in dry deposition". Atmos. Environ. 34: 2261-2282

Wild O., Fiore A.M., Shindell D.T., Doherty R.M., Collins W.J., et al., 2012, "Modelling future changes in surface ozone: a parameterized approach". Atmos. Chem. Phys. 12: 2037-2054

Wild O., 2007, "Modelling the global tropospheric ozone budget: exploring the variability in current models". Atmos. Chem. Phys. 7: 2643-2660

Williams E.R., 2009, "The global electrical circuit: A review". Atmos. Res., 91: 140-152.

Wilson R.C., Fleming Z. L., Monks P. S., Clain G., Henne S., et al., 2012, "Have primary emission reduction measures reduced ozone across Europe? An analysis of European rural background ozone trends 1996-2005".Atmos. Chem. Phys. 12: 437-454

Wittig V.E., Ainsworth E.A., Naidu S.L., Karnosky D.F., Long S.P., 2009, "Quantifying the impact of current and future tropospheric ozone on tree biomass, growth, physiology and biochemistry: a quantitative meta-analysis". Global Change Biol.15: 396-424

Wittig V.E., Ainsworth E.A., Long S.P., 2007,"To what extent do current and projected increases in surface ozone affect photosynthesis and stomatal conductance of trees? A meta-analytic review of the last 3 decades of experiments". Plant, Cell Environ. 30: 1150-1162

Xing J., Mathur R., Pleim J., C. Hogrefe, Gan C.M., et al., 2015, "Observations and modeling of air quality trends over 1990–2010 across the Northern Hemisphere: China, the United States and Europe". Atmos. Chem. Phys. 15: 2723-2747

Young P.J., Archibald A.T., Bowman K.W., Lamarque J.F., Naik V., et al., 2013, "Preindustrial to end 21st century projections of tropospheric ozone from the Atmospheric Chemistry and Climate Model Intercomparison Project (ACCMIP)". Atmos. Chem. Phys. 13: 2063-2090

Zak D.R., Pregitzer K.S., Kubiske M.E., Burton A.J., 2011, "Forest productivity under elevated CO_2 and O_3; positive feedbacks to soil N cycling sustain decade-long net primary productivity enhancement by CO_2. Ecology Letters 14: 1220-1226

Zeng G., Morgenstern O., Braesicke P., Pyle J.A., 2010, "Impact of stratospheric ozone recovery on tropospheric ozone and its budget". Geophys. Res. Lett. 37: L09805

Zeng G., Pyle J.A., Young P. J., 2008, "Impact of climate change on tropospheric ozone and its global budgets, Atmos. Chem. Phys. 8: 369-387

Zeng G. and Pyle J.A., 2003, "Changes in tropospheric ozone between 2000 and 2100 modeled in a chemistry-climate model". Geophys. Res. Lett. 30: 1392

Zhang Q., Streets D.G., Carmichael G.R., He K.B., Huo H., et al., 2009, "Asian emissions in 2006 for the NASA INTEX-B mission". Atmos. Chem. Phys. 9: 5131-5153

Zhang M.,Xu Y., Uno I., Akimoto H., 2004, "A numerical study of tropospheric ozone in the springtime in east Asia". Adv. Atmos. Sci. 21: 163-170

Atmos. Chem. Phys. Discuss., doi:10.5194/acp-2017-74, 2017
Manuscript under review for journal Atmos. Chem. Phys.
Discussion started: 9 March 2017

Atmospheric Chemistry and Physics Discussions

Zhang L., Brook J. R., Vet R., 2003, "A revised parameterization for gaseous dry deposition in air-quality models". Atmos. Chem. Phys. 3: 2067-2082

Zhu Z., Piao S., Myneni R.B., Huang M., Zeng Z., et al., 2016, "Greening of the Earth and its drivers". Nature Climate Change 6: 791-795

Figure 1: Surface ozone mean concentrations (in ppb) at the lower model layer for each ACCMIP model for the historical run and for RCP2.6, RCP4.5 and RCP8.5 simulations by 2100.

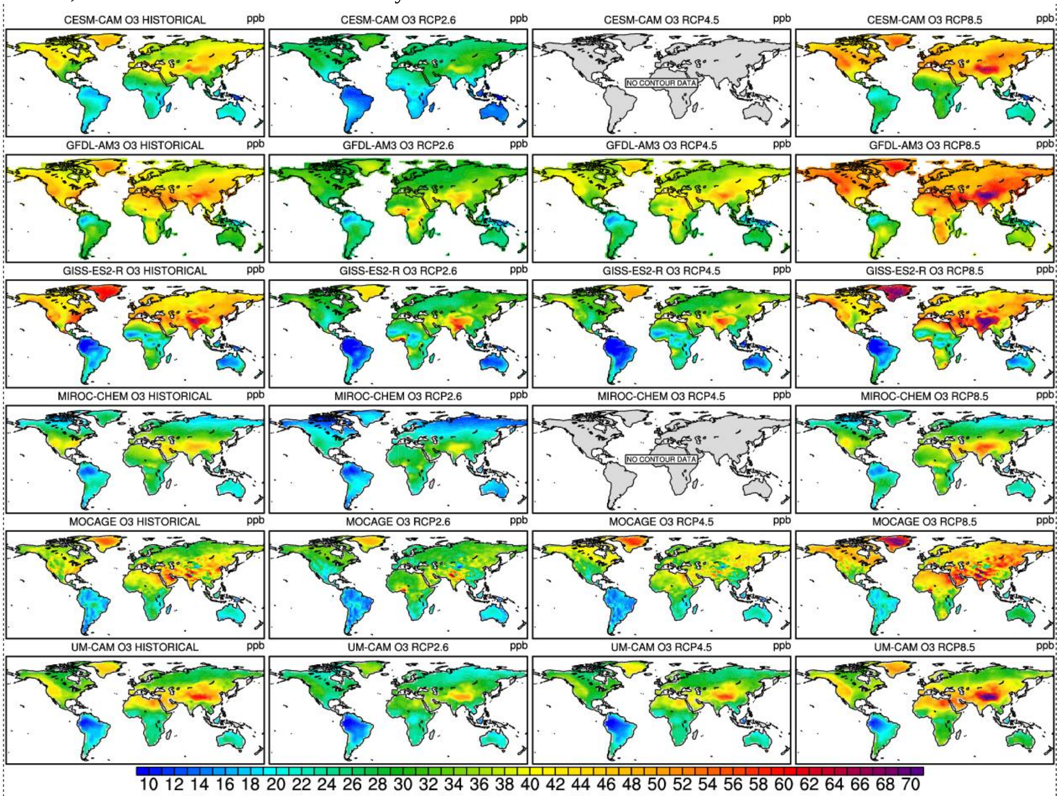

Figure 2: Surface AOT40 means (in ppm.h) at the lower model layer for each ACCMIP model for the historical run and for RCP2.6, RCP4.5 and RCP8.5 simulations by 2100.

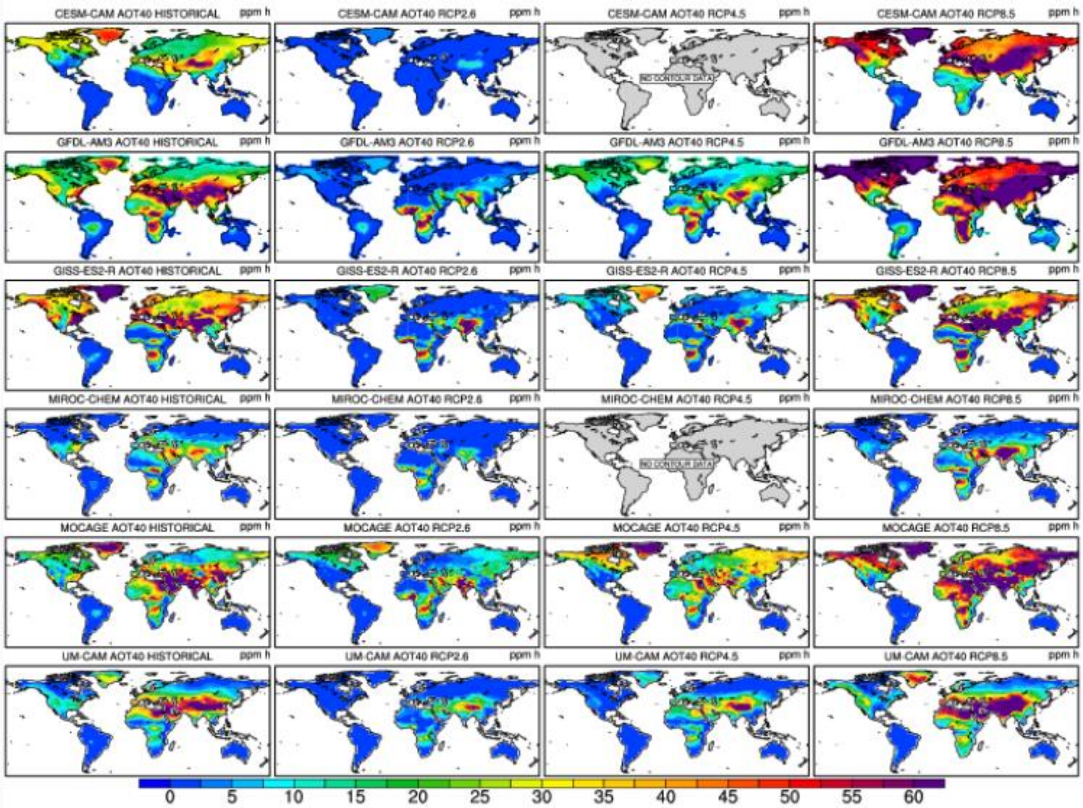

Figure 3: Simulated percentage changes (%) in the potential ozone impact on vegetation (IO3) for each ACCMIP model between RCP2.6, RCP4.5 and RCP8.5 simulations and the historical run.

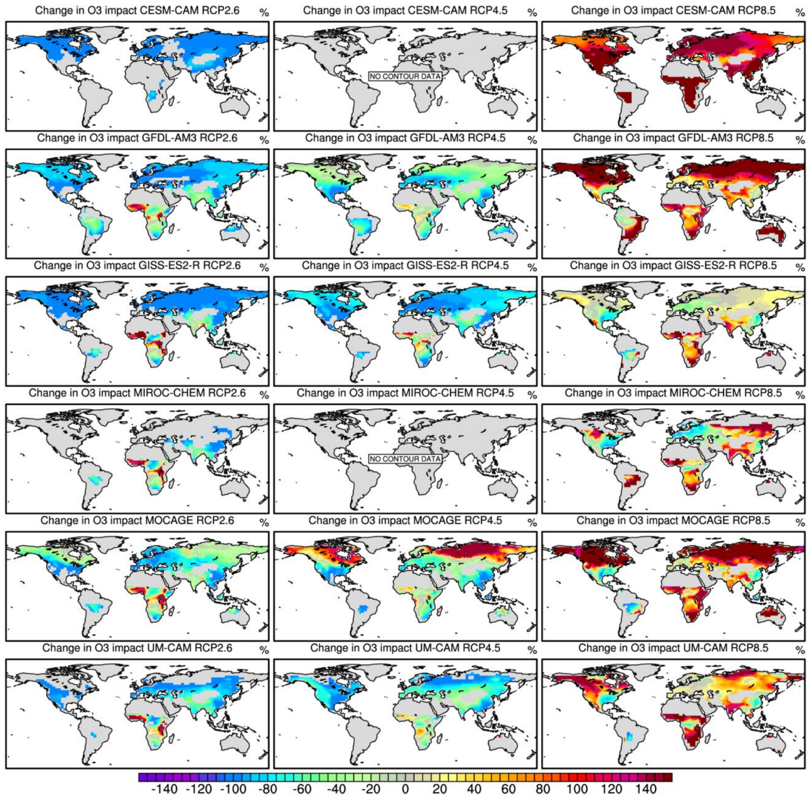

Atmos. Chem. Phys. Discuss., doi:10.5194/acp-2017-74, 2017
Manuscript under review for journal Atmos. Chem. Phys.
Discussion started: 9 March 2017

Table 1: Characteristics of the models, including simulation time slice, spatial resolution, simulated gas species and associated bibliographic references (from Lamarque et al., 2013 and Young et al. 2013). Black carbon (BC), Organic carbon (OC), Secondary Organic Aerosols (SOA), Dimethylsulfide (DMS), Chemistry Climate Model (CCM), Chemistry Transport Model (CTM), Chemistry-General Circulation Model (CGCM).

Models	**Type**	**Simulation length**	**Resolution (lat/lon)**	**Number of vertical pressure levels & top level**	**Species simulated**	**References**
CESM-CAM	CCM	2000-2009 and 2100-2109	1.875/2.5	26 levels 3.5 hPa	**16 gas species**; constant present-day isoprene, soil NOx, DMS and volcanic sulfur, oceanic CO.	Lamarque et al., 2012
GFDL-AM3	CCM	2001-2010 and 2101-2110	2.0/2.5	48 levels 0.017 hPa	**81 gas species**; SOx, BC, OC, SOA, NH_3, NO_3; constant pre-industrial soil NOx; constant present-day soil and oceanic CO, and biogenic VOC; climate-sensitive dust, sea salt, and DMS.	Donner et al., 2011 Naik et al., 2012
GISS-E2-R	CCM	2000-2004 and 2101-2105	2.0/2.5	40 levels 0.14 hPa	**51 gas species**; interactive sulfate, BC, OC, sea salt, dust, NO_3, SOA, alkenes; constant present-day soil NOx; climate-sensitive dust, sea salt, and DMS; climate-sensitive isoprene based on present-day vegetation.	Lee and Adams, 2011 Shindell et al., 2012
MIROC-CHEM	CCM	2000-2010 and 2100-2104	2.8/2.8	80 levels 0.003 hPa	**58 gas species**; SO_4, BC, OC; constant present-day VOCs, soil-NOx, oceanic-CO; climate-sensitive dust, sea salt and DMS.	Watanabe et al., 2011
MOCAGE	CTM	2000-2003 and 2100-2103	2.0/2.0	47 levels 6.9 hPa	**110 gas species**; constant present-day isoprene, other VOCs, oceanic CO and soil NOx.	Josse et al., 2004 Krinner et al., 2005 Teyssèdre et al., 2007
UM-CAM	CGCM	2000-2005 and 2094-2099	2.50/3.75	19 levels 4.6 hPa	**60 gas species**; constant present-day biogenic isoprene, soil NOx, biogenic and oceanic CO.	Zeng et al., 2008, 2010

Atmos. Chem. Phys. Discuss., doi:10.5194/acp-2017-74, 2017
Manuscript under review for journal Atmos. Chem. Phys.
Discussion started: 9 March 2017

Atmospheric Chemistry and Physics Discussions
Open Access

Table 2a: Annual total emissions of CO (Tg CO/year), NMVOCs (Tg C/year), NOx (Tg N/year, including lightning and soil NOx), total lightning NOx emissions (LNOx) and global atmospheric methane (CH_4) burden (Tg) for the historical simulations in each model (from Young et al., 2013 and * from Voulgarakis et al., 2013).

Models	**Historical**				
	CO	* CH_4	NMVOCs	NOx	*LNOx
CESM-CAM	1248	4902	429	50.0	4.2
GFDL-AM3	1246	4809	830	46.2	4.4
GISS-E2-R	1070	4793	830	48.6	7.7
MIROC-CHEM	1064	4805	833	57.3	9.7
MOCAGE	1168	4678	1059	47.9	5.2
UM-CAM	1148	4879	535	49.2	5.1

Table 2b: Simulated percentage (%) changes in total emissions of CO, NMVOCs, NOx (including lightning and soil NOx), total lightning NOx emissions (LNOx) and global atmospheric CH_4 burden for each model between 2100 and historical simulation for RCPs (from Young et al., 2013 and *Voulgarakis et al., 2013). The last row shows means and standard deviations (SD). Missing or not available data are identified (n.a).

Models	**RCP2.6 scenario**					**RCP4.5 scenario**					**RCP8.5 scenario**				
	CO	*CH_4	VOCs	NOx	*LNOx	CO	*CH_4	VOCs	NOx	*LNOx	CO	*CH_4	VOCs	NOx	*LNOx
CESM-CAM	- 36.7	- 27.1	0	- 52.8	+ 7.1	n.a	n.a	n.a	n.a	n.a	- 30.1	+ 112.1	0	- 33.0	+ 29.7
GFDL-AM3	- 36.9	- 27.9	- 5.0	- 47.0	+ 12.6	- 47.4	- 9.3	- 3.6	- 41.5	+ 23.5	- 30.3	+ 116.1	- 1.9	- 22.4	+ 38.2
GISS-E2-R	- 42.8	- 21.0	+ 0.5	- 44.2	+ 3.8	- 54.9	+ 4.6	+ 6.9	- 39.2	+ 12.2	- 35.1	+ 152.7	+ 19.8	- 20.0	+ 26.2
MIROC-CHEM	- 43.1	- 28.2	- 7.1	- 36.0	+ 7.5	n.a	n.a	n.a	n.a	n.a	- 35.4	+ 116.0	- 3.4	- 6.9	+ 38.0
MOCAGE	- 39.4	- 28.8	- 6.5	- 45.7	+ 5.2	n.a	n.a	n.a	n.a	n.a	- 32.3	+ 113.4	- 2.8	- 22.9	+ 19.9
UM-CAM	- 39.0	- 27.9	- 11.3	- 40.6	+ 8.1	- 50.4	- 8.7	- 9.2	- 36.0	+ 17.5	- 32.0	+ 112.1	- 4.2	- 17.2	+ 43.6
Mean ± SD	- 39.7 ± 2.2	- 26.8 ± 3.7	- 4.9 ± 4.9	- 44.4 ± 4.3	+ 7.4 ± 2.0	- 50.9 ± 3.2	- 4.5 ± 9.4	- 2.0 ± 11.4	- 38.9 ± 2.3	+ 17.7 ± 3.7	- 32.5 ± 1.8	+ 120.4 ± 19.5	+ 1.3 ± 11.6	- 20.4 ± 7.0	+ 32.6 ± 10.8

Table 3a: Global and hemispheric (averaged over the domain) surface ozone mean concentrations (in ppb) and AOT40 means (in ppm.h) for the historical simulations in each model (North and South Hemisphere, i.e NH and SH). The last row shows means and standard deviations (SD).

Models	Ozone conc. global	Ozone conc. SH	Ozone conc. NH	AOT40 global	AOT40 SH	AOT40 NH
CESM-CAM	31.3	20.9	36.4	12.8	0.2	18.9
GFDL-AM3	38.6	30.6	42.9	21.8	4.7	30.8
GISS-E2-R	35.8	22.3	42.3	26.0	3.6	36.8
MIROC-CHEM	27.9	20.4	31.4	7.3	1.9	9.8
MOCAGE	32.9	21.5	38.3	22.9	3.5	31.8
UM-CAM	31.3	21.4	36.0	14.4	1.3	20.6
Mean ± SD	33.0 ± 3.8	22.9 ± 3.8	37.9 ± 4.3	17.5 ± 7.2	2.5 ± 1.7	24.8 ± 10.1

Table 3b: Simulated percentage (%) changes in global and hemispheric surface ozone mean concentrations and in global mean stratospheric ozone column (* from Voulgarakis et al., 2013) for each model between 2100 and historical simulation for RCPs (North and South Hemisphere, i.e NH and SH). The last row shows means and standard deviations (SD). Missing or not available data are identified (n.a).

Models	Surface ozone mean concentrations									* Stratospheric ozone		
	RCP2.6 global	RCP2.6 SH	RCP2.6 NH	RCP4.5 global	RCP4.5 SH	RCP4.5 NH	RCP8.5 global	RCP8.5 SH	RCP8.5 NH	RCP2.6 global	RCP4.5 global	RCP8.5 global
CESM-CAM	- 29.1	- 20.6	- 31.3	n.a	n.a	n.a	+ 21.9	+ 22.5	+ 20.5	n.a	n.a	+ 5.3
GFDL-AM3	- 20.5	- 10.8	- 24.5	- 11.7	- 6.9	- 13.5	+ 15.5	+ 18.6	+ 14.5	+ 3.3	+ 3.9	+ 8.4
GISS-E2-R	- 23.5	- 5.8	- 27.9	- 20.4	- 6.3	- 23.9	+ 7.0	+ 19.3	+ 3.8	+ 8.0	+ 8.8	+ 15.1
MIROC-CHEM	- 23.3	- 12.3	- 26.8	n.a	n.a	n.a	+ 3.9	+ 10.3	+ 2.2	+ 2.6	n.a	+ 4.2
MOCAGE	- 12.8	+ 7.4	- 18.5	- 1.8	+ 17.7	- 7.0	+ 23.1	+ 40.4	+ 16.7	+ 19.9	n.a	+ 23.6
UM-CAM	- 17.3	- 4.7	- 21.1	- 8.3	+ 0.9	- 10.8	+ 14.4	+ 24.3	+ 11.4	+ 6.7	+ 6.9	+ 7.4
Mean ± SD	- 21.1 ± 5.6	- 7.8 ± 9.4	- 25.0 ± 4.7	- 10.5 ± 7.7	+ 1.4 ± 11.5	- 13.8 ± 7.2	+ 13.8 ± 7.1	+ 22.6 ± 10.0	+ 11.5 ± 7.3	+ 8.1 ± 7.0	+ 6.5 ± 2.5	+ 10.7 ± 7.4

Table 3c: Simulated percentage (%) changes in global and hemispheric AOT40 means for each model between 2100 and historical simulation for RCPs (North and South Hemisphere, i.e NH and SH). Missing or not available data are identified (n.a).

Models	AOT40								
	RCP2.6 global	**RCP2.6 SH**	**RCP2.6 NH**	**RCP4.5 global**	**RCP4.5 SH**	**RCP4.5 NH**	**RCP8.5 global**	**RCP8.5 SH**	**RCP8.5 NH**
CESM-CAM	- 96.9	- 99.9	- 96.8	n.a	n.a	n.a	+ 138.3	+ 150.0	+ 134.9
GFDL-AM3	- 75.2	- 25.5	- 78.9	- 53.2	- 36.2	- 54.5	+ 96.3	+ 242.5	+ 85.1
GISS-E2-R	- 78.1	- 13.9	- 81.2	- 75.0	- 27.8	- 77.2	+ 22.3	+ 83.3	+ 19.5
MIROC-CHEM	- 74.0	- 10.5	- 80.6	n.a	n.a	n.a	+ 20.5	+ 78.9	+ 16.3
MOCAGE	- 53.7	+ 68.6	- 59.7	- 17.5	+ 202.9	- 28.3	+ 85.1	+ 448.6	+ 67.0
UM-CAM	- 73.6	+ 92.3	- 76.7	- 52.8	+7.7	- 54.8	+ 49.3	+ 176.9	+ 45.1
Mean ± SD	- 75.2 ± 13.7	+ 1.9 ± 69.5	- 79.0 ± 11.8	- 49.6 ± 23.8	+ 36.6 ± 112.4	- 53.7 ± 20.0	+ 68.6 ± 46.3	+ 196.7 ± 137.7	+ 61.3 ± 44.8

Table 3d: Simulated percentage (%) changes in potential O_3 impact on vegetation (IO3) for each model between 2100 and historical simulation for RCPs (North and South Hemisphere, i.e NH and SH).Missing or not available data are identified (n.a).

Models	Risk factor IO3								
	RCP2.6 global	**RCP2.6 SH**	**RCP2.6 NH**	**RCP4.5 global**	**RCP4.5 SH**	**RCP4.5 NH**	**RCP8.5 global**	**RCP8.5 SH**	**RCP8.5 NH**
CESM-CAM	- 97.2	- 91.8	-97.5	n.a	n.a	n.a	+ 129.6	+146.8	+127.5
GFDL-AM3	- 69.4	- 49.1	- 74.8	- 50.1	- 61.1	- 47.2	+ 91.9	+95.5	+90.4
GISS-E2-R	- 66.1	- 20.7	- 74.3	- 71.7	- 53.3	- 74.6	+ 21.5	+56.6	+14.2
MIROC-CHEM	- 41.4	- 18.9	- 51.9	n.a	n.a	n.a	+ 41.0	+103.8	+25.5
MOCAGE	- 46.6	-22.8	- 51.4	- 7.0	- 38.0	- 1.0	+ 77.7	+68.2	+80.0
UM-CAM	- 45.8	- 9.2	- 71.3	- 59.5	+ 2.0	- 69.0	+ 61.3	+84.2	+56.0
Mean ± SD	- 61.1 ± 21.1	- 35.5 ± 30.7	- 70.2 ± 17.2	- 47.1 ± 28.1	- 37.6 ± 28.1	- 47.9 ± 33.4	+ 70.5 ± 38.4	+ 92.5 ± 31.7	+ 65.6 ± 42.4